Modeling of General Constitutive Relationships in SCN TLM

Leonardo R. A. X. de Menezes, *Member, IEEE*, and Wolfgang J. R. Hoefer, *Fellow, IEEE*

***Abstract*— The modeling of general constitutive relationships in SCN (symmetrical condensed node) TLM is presented. The technique consists of decoupling the impulse scattering at the nodes from equations describing the medium by using equivalent node sources with state-variable formulation of the constitutive relationships. The procedure requires few modifications of TLM. Numerical examples are presented.**

I. Introduction

IN THE BASIC TLM formulation, dielectric permittivity and magnetic permeability are modeled by open and short circuited stubs which are connected to the nodes; the characteristic admittance of the stubs is a function of the constitutive parameters [1]. This method is very robust and most appropriate when and are constants. However when the material constitutive parameters are frequency dispersive and nonlinear, the representation by hard-wired stubs becomes computationaly difficult and uneconomical because a modification in time of the stub admittances leads to a modification of the impulse scattering matrix of the node.

A better way is to decouple the impulse scattering at the nodes from the equations describing the behavior of the medium by representing the latter by a differential equation or equivalent lumped element network and connecting it to each node by a transmission line of infinitesimal length and characteristic admittance equal to the driving point admittance of the node [2]–[4].

The procedure presented in this paper is an efficient TLM representation of arbitrary constitutive relationships. Using decoupled scattering matrices with equivalent node sources (Thevenin and Norton equivalents of the node), the constitutive equations are expressed in a generic formulation allowing the inclusion of arbitrary medium behavior in TLM models. The resulting equations are solved with the state-variable approach.

II. Theory

This section is divided into four parts. The first describes the modeling of arbitrary dielectric and magnetic materials in two-dimensional (2-D) shunt and series TLM networks. In the second part, the method is extended to three-dimensional (3-D) SCN TLM. In the third part, the networks describing the medium behavior are formulated in terms of equivalent node sources, and in the fourth part the resulting differential equations are expressed and solved using the state-space approach.

Manuscript received June 10, 1995; revised February 15, 1996. This work was supported in part by the Brazilian Government agency Conselho Nacional de Pesquisa (CNPq).

The authors are with NSERC/MPR Teltech Research Chair in RF Engineering, Department of Electrical and Computer Engineering, University of Victoria, Victoria B.C., Canada.

Publisher Item Identifier S 0018-9480(96)03804-5.

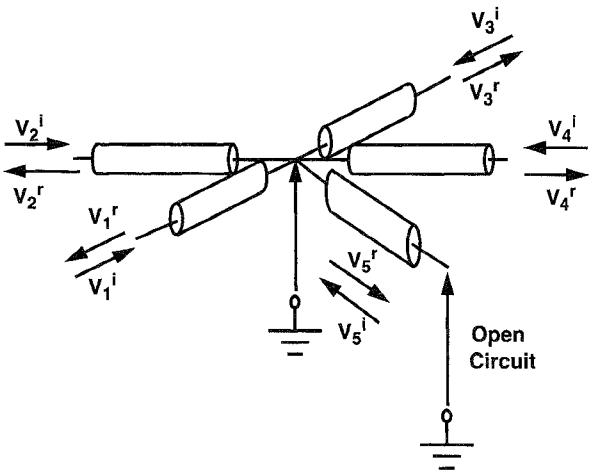

Fig. 1. Two-dimensional TLM shunt node N1.

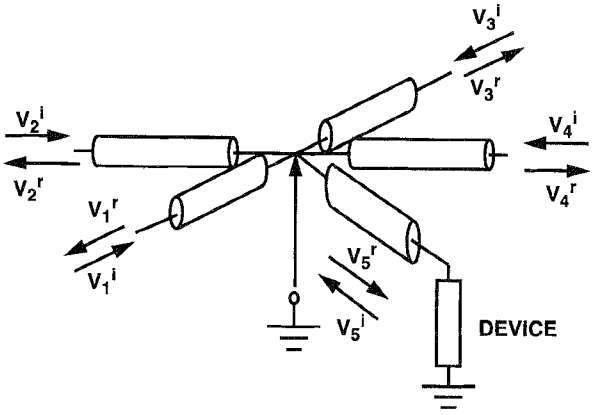

Fig. 2 Two-dimensional TLM shunt node N2

A. Two-Dimensional TLM Formulation

General isotropic materials can be modeled in 2-D-TLM by reactively loading each node of the network. As mentioned above, the reactive load can be either modeled by a reactive stub (Fig. 1) or by a reactive lumped element network (Fig. 2). The latter formulation will now be given for general nondispersive linear media, for the sake of simplicity.

Since the characteristics of shunt and series-connected TLM networks are related to each other by duality, we will only

derive the formulation for the shunt case and simply state the analogous results for the series case.

In the shunt connected TLM cell the reactive network across the node models the polarization of the medium in the presence of an electric field, and the current flowing through it is the polarization current. The equations relating this current to the electric field describe the dielectric response of the medium.

Maxwell's second curl equation in two dimensions ($\partial/\partial y = 0$)

$$\frac{\partial H_x}{\partial z} - \frac{\partial H_z}{\partial x} = \epsilon_0 \epsilon_r \frac{\partial E_y}{\partial t} \tag{1}$$

is modeled by the shunt type 2-D-TLM network as

$$-\frac{\partial i_z}{\partial z} - \frac{\partial i_x}{\partial x} = (2C_0 + C_p)\frac{\partial v_y}{\partial t} \tag{2}$$

with the equivalences

$$i_z \equiv -H_x \quad i_x \equiv H_z \quad v_y \equiv E_y$$
$$\epsilon_0 \equiv 2C_0 \quad \epsilon_r \equiv 2C_0 + C_p$$

where C_0 is the capacitance per unit length of the link lines.

For a square cell with $\Delta x = \Delta z = \Delta l$the total displacement current is thus

$$i_d = i_{d0} + i_p = 2C_0 \Delta l \frac{\partial v_y}{\partial t} + C_p \Delta l \frac{\partial v_y}{\partial t} \tag{3}$$

where i_d is the total displacement current, i_{do} is the displacement current *in vacuo* and i_p is the polarization current in the medium.

The equivalence between

$$\epsilon_0 \epsilon_r = \epsilon_0(1 + \chi) = \epsilon_0[1 + (\epsilon_r - 1)]$$

and

$$2C_0 + C_p = 2C_0\left(1 + \frac{C_p}{2C_0}\right)$$

yields with $\epsilon_0 \equiv 2C_0$

$$C_p = 2C_0\chi = 2C_0(\epsilon_r - 1)$$

obtaining for the polarization current in (3)

$$i_p = 2C_0(\epsilon_r - 1)\Delta l \frac{\partial v_y}{\partial t}. \tag{4}$$

Furthermore

$$C_0 = \sqrt{\frac{C_0}{L_0}}\sqrt{L_0 C_0} = \frac{Y_0}{c} = \frac{Y_0 \Delta t}{\Delta l} \tag{5}$$

where L_0 and Y_0 are the inductance per unit length and the characteristic admittance of the link lines, respectively, Δt is the timestep, and c the speed of light (on the link lines). Hence

$$i_p = 2\frac{Y_0 \Delta l}{c}(\epsilon_r - 1)\frac{\partial v_y}{\partial t} = \left(2\frac{Y_0 \Delta l}{c}\right)\frac{\partial p_y}{\partial t} \tag{6}$$

where p_y is the normalized polarization

$$p_y \equiv P_y/\epsilon_0.$$

The shunt reactance connected to the node is usually described by a current-voltage relationship. In order to connect it with the scattering mechanism in the TLM network, the total voltage and current across the reactance must be expressed in terms of incident and reflected voltage impulses. To this end, the shunt reactance is connected to the node via a transmission line of infinitesimal length and characteristic admittance Y_s. In order to avoid multiple reflections on this line, Y_s is matched to the driving point admittance of the node, i.e. $Y_s = 4Y_0$, where Y_0 is characteristic admittance of the link lines.

The voltage and current across the shunt reactance can thus be related to the voltage impulses incident and reflected at the node on this transmission line as follows:

$$v_y = v_{ey}^r + v_{ey}^i$$
$$i_p = 4Y_0(v_{ey}^r - v_{ey}^i). \tag{7}$$

The scattering matrix of the node is

$$\begin{bmatrix} v_1 \\ v_2 \\ v_3 \\ v_4 \end{bmatrix}^r = \frac{1}{4}\begin{bmatrix} -3 & 1 & 1 & 1 \\ 1 & -3 & 1 & 1 \\ 1 & 1 & -3 & 1 \\ 1 & 1 & 1 & -3 \end{bmatrix}\begin{bmatrix} v_1 \\ v_2 \\ v_3 \\ v_4 \end{bmatrix}^i + \begin{bmatrix} v_{ey} \\ v_{ey} \\ v_{ey} \\ v_{ey} \end{bmatrix}^i \tag{8}$$

and the reflected voltage v_{ey}^r is calculated as

$$v_{ey}^r = \tfrac{1}{4}(v_1^i + v_2^i + v_3^i + v_4^i). \tag{9}$$

Therefore, the incident voltage v_{ey}^i used in (8) is calculated using (9) with (7) and (6).

In the series node case, the decoupled scattering matrix is

$$\begin{bmatrix} v_1 \\ v_2 \\ v_3 \\ v_4 \end{bmatrix}^r = \frac{1}{4}\begin{bmatrix} 3 & 1 & 1 & -1 \\ 1 & 3 & -1 & 1 \\ 1 & -1 & 3 & 1 \\ -1 & 1 & 1 & 3 \end{bmatrix}\begin{bmatrix} v_1 \\ v_2 \\ v_3 \\ v_4 \end{bmatrix}^i + \frac{1}{4}\begin{bmatrix} -1 & 0 & 0 & 0 \\ 0 & 1 & 0 & 0 \\ 0 & 0 & 1 & 0 \\ 0 & 0 & 0 & -1 \end{bmatrix}\begin{bmatrix} v_m \\ v_m \\ v_m \\ v_m \end{bmatrix}^i$$
$$v_m^r = (-v_1^i + v_2^i + v_3^i - v_4^i). \tag{10}$$

The current and voltage over the node are defined as

$$v_{\text{mag}}(t) = v_m^t(t) + v_m^i(t)$$
$$i(t) = \frac{v_m^r(t) - v_m^i(t)}{4Z_0} \tag{11}$$

and the magnetization vector is

$$v_{\text{mag}}(t) = \left(2\frac{Z_0 \Delta l}{c}\right)\frac{d}{dt}m(t) \tag{12}$$

where (in the linear nondispersive case) $m(t) = (\mu_r - 1)i(t)$ is the normalized magnetization vector, $v_{\text{mag}}(t)$ is the magnetization voltage and $v_n^r(t), v_n^i(t)$ are the reflected and incident voltages at the input port of the network modeling the magnetic behavior of the medium.

B. Obtention of the SCN Formulation

The SCN formulation is obtained by combining 2-D shunt and series nodes [6]. These nodes are decoupled from the medium using the procedure described in Section II-A. The resulting medium constitutive equations are

$$
\begin{aligned}
i_{\text{pol}x} &= \left(2\frac{Y_0\Delta l}{c}\right)\frac{dp_x}{dt} \quad v_{\text{mag}x} = \left(2\frac{Z_0\Delta l}{c}\right)\frac{dm_x}{dt}\\
p_x(t) &= P_x(t)\frac{\Delta l}{2\epsilon_0} \quad m_x(t) = M_x(t)\frac{\Delta l}{2}\\
i_{\text{pol}y} &= \left(2\frac{Y_0\Delta l}{c}\right)\frac{dp_y}{dt} \quad v_{\text{mag}y} = \left(2\frac{Z_0\Delta l}{c}\right)\frac{dm_y}{dt}\\
p_y(t) &= P_x(t)\frac{\Delta l}{2\epsilon_0} \quad m_y(t) = M_y(t)\frac{\Delta l}{2}\\
i_{\text{pol}z} &= \left(2\frac{Y_0\Delta l}{c}\right)\frac{dp_z}{dt} \quad v_{\text{mag}z} = \left(2\frac{Z_0\Delta l}{c}\right)\frac{dm_z}{dt}\\
p_z(t) &= P_z(t)\frac{\Delta l}{2\epsilon_0} \quad m_z(t) = M_z(t)\frac{\Delta l}{2}
\end{aligned}
\tag{13}
$$

$$
\begin{aligned}
i_{\text{pol}x} &= Y_r(v^t_{ex} - v^i_{ex}) \quad v_x = v^t_{ex} + v^i_{ex}\\
p_x &= p_x(v_x, v_y, v_z, i_x, i_y, i_z)\\
i_{\text{pol}y} &= Y_r(v^t_{ey} - v^i_{ey}) \quad v_y = v^t_{ey} + v^i_{ey}\\
p_y &= p_x(v_x, v_y, v_z, i_x, i_y, i_z)\\
i_{\text{pol}z} &= Y_r(v^t_{ez} - v^i_{ez}) \quad v_z = v^t_{ez} + v^i_{ez}\\
p_z &= p_x(v_x, v_y, v_z, i_x, i_y, i_z)\\
v_{\text{mag}x} &= v^r_{mx} + v^i_{mx} \quad i_x = (v^r_{mx} - v^i_{mx})/Z_r\\
m_x &= m_x(v_x, v_y, v_z, i_x, i_y, i_z)\\
v_{\text{mag}y} &= v^r_{my} + v^i_{my} \quad i_y = (v^r_{my} - v^i_{my})/Z_r\\
m_y &= m_y(v_r, v_y, v_z, i_x, i_y, i_z)\\
v_{\text{mag}zx} &= v^r_{mzx} + v^i_{mzx} \quad i_z x = (v^r_{mzx} - v^i_{mzx})/Z_r\\
m_z x &= m_z x(v_x, v_y, v_z, i_x, i_y, i_z)
\end{aligned}
\tag{14}
$$

the reflected voltages on branches 1–12 are calculated using [6], with the same numbering scheme used in [7]

$$
\begin{aligned}
v^r_1 &= v_x(t) - Z_r i_z(t) - v^i_{12} \quad v^r_5 = v_z(t) + Z_r i_x(t) - v^i_7(t)\\
v^r_9 &= v_x(t) - Z_r i_y(t) - v^i_2 \quad v^r_2 = v_x(t) + Z_r i_y(t) - v^i_9\\
v^r_6 &= v_z(t) - Z_r i_y(t) - v^i_{10} \quad v^r_{10} = v_z(t) + Z_r i_y(t) - v^i_6\\
v^r_3 &= v_y(t) + Z_r i_z(t) - v^i_{11} \quad v^r_7 = v_z(t) - Z_r i_x(t) - v^i_5\\
v^r_{11} &= v_y(t) - Z_r i_z(t) - v^i_3 \quad v^r_4 = v_y(t) - Z_r i_x(t) - v^i_8\\
v^r_8 &= v_y(t) + Z_r i_x(t) - v^i_4 \quad v^r_{12} = v_x(t) + Z_r i_z(t) - v^i_1
\end{aligned}
\tag{15}
$$

with $Y_r/Y_0 = Z_r/Z_0 = 4$ and

$$
\begin{aligned}
v_x(t) &= (v^i_1(t) + v^i_2(t) + v^i_9(t) + v^i_{12}(t))/4 + v^i_{ex}(t)\\
v_y(t) &= (v^i_3(t) + v^i_4(t) + v^i_8(t) + v^i_{11}(t))/4 + v^i_{ey}(t)\\
v_z(t) &= (v^i_5(t) + v^i_6(t) + v^i_7(t) + v^i_{10}(t))/4 + v^i_{ez}(t)\\
i_x(t) &= (v^i_4(t) - v^i_5(t) + v^i_7(t) - v^i_8(t)) - v^i_{mx}(t))/4\\
i_y(t) &= (v^i_6(t) - v^i_2(t) + v^i_9(t) - v^i_{10}(t)) - v^i_{my}(t))/4\\
i_z(t) &= (v^i_1(t) - v^i_3(t) + v^i_{12}(t) - v^i_{11}(t)) - v^i_{mz}(t))/4.
\end{aligned}
\tag{16}
$$

The conditions (15) to (16) can be expressed in the system

$$
[v^r] = [S][v^i] + \tfrac{1}{4}[v^i_s] \quad [v^r_s] = [T][v^i] \tag{17}
$$

where, as shown in (18) and (19) at the bottom of the page, and

$$
\begin{aligned}
[v^r_s] &= [v^r_{ex} v^r_{ey} v^r_{ez} 4v^r_{mx} 4v^r_{my} 4v^r_{mz}]^t\\
[v^i_s] &= [4v^r_{ex} 4v^r_{ey} 4v^r_{ez} - v^r_{mx} - v^r_{my} - v^r_{mz}]^t
\end{aligned}
\tag{20}
$$

and the subscript t denotes the transpose vector.

The reflected voltages v^r_m and v^r_e are calculated as follows:

$$
\begin{aligned}
v^r_{ex} &= \tfrac{1}{4}(v^i_1 + v^i_2 + v^i_9 + v^i_{12}) \quad v^r_{mx} = (v^i_4 - v^i_5 + v^i_7 - v^i_8)\\
v^r_{ey} &= \tfrac{1}{4}(v^i_3 + v^i_4 + v^i_8 + v^i_{11}) \quad v^r_{my} = (v^i_6 - v^i_2 + v^i_9 - v^i_{10})\\
v^r_{ez} &= \tfrac{1}{4}(v^i_5 + v^i_6 + v^i_7 + v^i_{10}) \quad v^r_{mz} = (v^i_1 - v^i_3 - v^i_{12} + v^i_{11}).
\end{aligned}
\tag{21}
$$

$$
[S] = \tfrac{1}{4}\begin{bmatrix}
0 & 1 & 1 & 0 & 0 & 0 & 0 & 0 & 1 & 0 & -1 & -2\\
1 & 0 & 0 & 0 & 0 & 1 & 0 & 0 & -2 & -1 & 0 & 1\\
1 & 0 & 0 & 1 & 0 & 0 & 0 & 1 & 0 & 0 & -2 & -1\\
0 & 0 & 1 & 0 & 1 & 0 & -1 & -2 & 0 & 0 & 1 & 0\\
0 & 0 & 0 & 1 & 0 & 1 & -2 & -1 & 0 & 1 & 0 & 0\\
0 & 1 & 0 & 0 & 1 & 0 & 1 & 0 & -1 & -2 & 0 & 0\\
0 & 0 & 0 & -1 & -2 & 1 & 0 & 1 & 0 & 1 & 0 & 0\\
0 & 0 & 1 & -2 & -1 & 0 & 1 & 0 & 0 & 0 & 1 & 0\\
1 & -2 & 0 & 0 & 0 & -1 & 0 & 0 & 0 & 1 & 0 & 1\\
0 & -1 & 0 & 0 & 1 & -2 & 1 & 0 & 1 & 0 & 0 & 0\\
-1 & 0 & -2 & 1 & 0 & 0 & 0 & 1 & 0 & 0 & 0 & 1\\
-2 & 1 & -1 & 0 & 0 & 0 & 0 & 0 & 1 & 0 & 1 & 0
\end{bmatrix}
\tag{18}
$$

$$
[T] = \tfrac{1}{4}\begin{bmatrix}
1 & 1 & 0 & 0 & 0 & 0 & 0 & 0 & 1 & 0 & 0 & 1\\
0 & 0 & 1 & 1 & 0 & 0 & 0 & 1 & 0 & 0 & 1 & 0\\
0 & 0 & 0 & 0 & 1 & 1 & 1 & 0 & 0 & 1 & 0 & 0\\
0 & 0 & 0 & 1 & -1 & 0 & 1 & -1 & 0 & 0 & 0 & 0\\
0 & -1 & 0 & 0 & 0 & 1 & 0 & 0 & 1 & -1 & 0 & 0\\
1 & 0 & -1 & 0 & 0 & 0 & 0 & 0 & 0 & 0 & 1 & -1
\end{bmatrix}
\tag{19}
$$

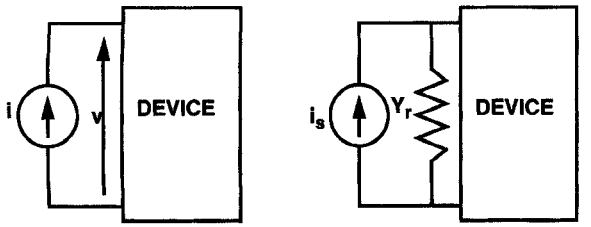

Fig. 3. Norton equivalent source of the node (dielectric behavior).

The link between the incident and reflected vectors given in (20) is obtained by (13) and (14).

C. The Equivalent Node Sources

The disadvantage of the substitution of (14) into (13) and subsequent discretization of the resulting expression is the loss of flexibility of the constitutive relationships modeling, since in this approach the final discretized expression will be different according to the medium equations. Therefore, it is important to deduce a robust solution procedure that enables (13) to be used independently of the constitutive equation. This is done considering the Norton and Thevenin circuit equivalent of the node as sources connected to the networks.

The voltage and current on the input port of each network can be expressed as

1) Shunt network:

$$i_{\mathrm{pol}}(t) = 2Y_r v_e^r(t) - Y_r v(t) \quad v_e^i(t) = v(t) - v_e^r(t). \tag{22}$$

2) Series network:

$$v_{\mathrm{mag}}(t) = 2Z_r v_m^r(t) - Z_r i(t) \quad v_m^i(t) = -(4i(t) - v_m^r(t)). \tag{23}$$

These equations can be rearranged and substituted into (13) resulting in

$$\begin{aligned} i_s(t) &= 2Y_r v_e^r(t) = Y_0 2\frac{\Delta l}{c}\frac{d}{dt}p(t) + Y_r v(t) \\ v_s(t) &= 2Z_r v_m^r(t) = Z_0 2\frac{\Delta l}{c}\frac{d}{dt}m(t) + Z_r i(t). \end{aligned} \tag{24}$$

The representation of (24) in the equivalent circuit form for the polarization is shown in Fig. 3.

Applying the same procedure to all directions, the equivalent current sources are obtained from the polarization current i_{pol} and the total voltage across the node $v(t)$, while the equivalent voltage sources are deduced from the magnetization voltage v_{mag} and total current over the node $i(t)$

$$\begin{aligned} i_{sx}(t) &= 2Y_r v_{ex}^r(t) = 8v_{ex}^r(t) = \frac{2\Delta l}{d}\frac{d}{dt}p_x(t) + 4v_x(t) \\ i_{sy}(t) &= 2Y_r v_{ey}^r(t) = 8v_{ey}^r(t) = \frac{2\Delta l}{d}\frac{d}{dt}p_y(t) + 4v_y(t) \\ i_{sz}(t) &= 2Y_r v_{ez}^r(t) = 8v_{ez}^r(t) = \frac{2\Delta l}{d}\frac{d}{dt}p_z(t) + 4v_z(t) \\ v_{sx}(t) &= 2Z_r v_{mx}^r(t) = 8v_{mx}^r(t) = \frac{2\Delta l}{d}\frac{d}{dt}m_x(t) + 4i_x(t) \\ i_{sy}(t) &= 2Z_r v_{my}^r(t) = 8v_{my}^r(t) = \frac{2\Delta l}{d}\frac{d}{dt}m_y(t) + 4i_y(t) \end{aligned}$$

$$i_{sz}(t) = 2Z_r v_{mz}^r(t) = 8v_{mz}^r(t) = \frac{2\Delta l}{d}\frac{d}{dt}m_z(t) + 4i_z(t). \tag{25}$$

The sources are calculated at each timestep by

$$\begin{aligned} i_{sx}(t) &= 2(v_1^i(t) + v_2^i(t) + v_9^i(t) + v_{12}^i(t)) \\ i_{sy}(t) &= 2(v_3^i(t) + v_4^i(t) + v_8^i(t) + v_{11}^i(t)) \\ i_{sz}(t) &= 2(v_5^i(t) + v_6^i(t) + v_7^i(t) + v_{10}^i(t)) \\ v_{sx}(t) &= 8(v_4^i(t) - v_5^i(t) + v_7^i(t) - v_8^i(t)) \\ v_{sy}(t) &= 8(v_6^i(t) - v_2^i(t) + v_9^i(t) - v_{10}^i(t)) \\ v_{sz}(t) &= 8(v_1^i(t) - v_3^i(t) - v_{12}^i(t) + v_{11}^i(t)). \end{aligned} \tag{26}$$

The solution of (26), (25), and (15) will result in the reflected voltages in lines 1–12. The propagation between nodes is not affected. The incident voltages (20) can be calculated using the results from (25) substituted into (14). This procedure is applicable to all kinds of constitutive relationships. The adaptation to usual TLM programs, [7], is done by setting $Y_x = Y_y = Y_z = Z_x = Z_y = Z_z = 4$, obtaining the reflected voltages for the stubs, using (25) and (14) to obtain the incident voltages from the stubs, and then calculating the reflected voltages in branches 1–12 with the scattering matrix (18).

D. The State-Variable Approach

The use of equivalent node sources allows the solution of the network using nodal or Tableau analysis, [9]. Therefore, a SPICE circuit simulator could be used to solve the network at all nodes at each timestep. The problem of this approach is the need to formulate an equivalent circuit of the medium. Although this may be an easy task for most linear dispersive isotropic materials, that is certainly not the case for an arbitrary constitutive relationship.

However, the state-variable formulation of the constitutive relationship equations avoids this problem. In this approach, the use of equivalent circuits to model the constitutive relationships is not discarded but it is not necessary, since the state-equations can be obtained directly from nonlinear differential equations. The state-variable technique is easily incorporated into the TLM simulator without loss of generality. A general procedure for linear differential equations shown in [5] is outlined for a medium described by a fourth-order linear differential equation

$$a\frac{d^4 f}{dt^4} + b\frac{d^3 f}{dt^3} + c\frac{d^2 f}{dt^2} + d\frac{df}{dt} + ef = g \tag{27}$$

resulting in

$$\begin{aligned} \frac{d}{dt}\begin{bmatrix} x_1(t) \\ x_2(t) \\ x_3(t) \\ x_4(t) \end{bmatrix} &= \frac{1}{a}\begin{bmatrix} -b & 1 & 0 & 0 \\ -c & 0 & 1 & 0 \\ -d & 0 & 0 & 1 \\ -e & 0 & 0 & 0 \end{bmatrix}\begin{bmatrix} x_1(t) \\ x_2(t) \\ x_3(t) \\ x_4(t) \end{bmatrix} \\ &\quad + \begin{bmatrix} 0 & 0 & 0 & 0 \\ 0 & 0 & 0 & 0 \\ 0 & 0 & 0 & 0 \\ 0 & 0 & 0 & \frac{1}{a} \end{bmatrix}\begin{bmatrix} 0 \\ 0 \\ 0 \\ g(t) \end{bmatrix} \end{aligned} \tag{28}$$

where $x_1(t) = f(t)$.

The resulting equations can be solved either analytically or numerically. The analytical solution of (28) would result in a discretized convolution procedure, restricting the use of the formulation to linear materials, since the convolution procedure requires the linearity of the system. If the numerical approach is used, several discretization schemes may be chosen. However, there are two major schemes that are very attractive, for reasons of stability and efficiency:

1) Backward Euler scheme [10]
2) Approximate Trapezoidal scheme (or first order Padé approximant)

The first scheme introduces losses in the final result, but there is no frequency shift, and it is very simple to implement. The second scheme is far more precise than the former, conserves energy and uses the same kind of discretization as used in TLM, Therefore, for linear isotropic nondispersive materials, the results given by this approach and usual TLM are virtually indistinguishable.

Both schemes transform the continuous state equations

$$\frac{d}{dt}[x(t)] = [A][x(t)] + [B][u(t)]$$
$$[y(t)] = [C][x(t)] + [D][u(t)] \tag{29}$$

into the discretized form

$$[x(t+\Delta t)] = [P][x(t)] + [Q][u(t)] + [R][x(t-\Delta t)]$$
$$[y(t+\Delta t)] = [C][x(t+\Delta t)] + [D][u(t+\Delta t)]. \tag{30}$$

The matrices $[P]$, $[Q]$, and $[R]$ will depend on the discretization scheme

1) Backward Euler scheme:

$$[P] = ([U] - \Delta t[A])^{-1}$$
$$[Q] = ([U] - \Delta t[A])^{-1}\Delta t[B]$$
$$[R] = [0] \tag{31}$$

where $[U]$ is the $n \times n$ identity matrix, and [0] is the null matrix.

2) Approximate trapezoidal scheme:

$$[P] = ([U] - \Delta t[A])^{-1}([U] + \Delta t[A])$$
$$[Q] = ([U] - \Delta t[A])^{-1}\frac{\Delta t}{2}[B]$$
$$[R] = ([U] - \Delta t[A])^{-1}\frac{\Delta t}{2}[B]. \tag{32}$$

III. Formulation of the State-Variable Equations

This section shows the implementation of the state-variable equations for several kinds of media. The presented results are the continuous state-variable equations.

A. Linear isotropic nondispersive medium

In this case

$$v_s(t) = 2Z_r v_m^r(t) = Z_0(\mu_r - 1)2\frac{\Delta l}{c}\frac{d}{dt}i(t) + Z_r i(t)$$
$$i_s(t) = 2Y_r v_e^r(t) = Y_0(\epsilon_r - 1)2\frac{\Delta l}{c}\frac{d}{dt}v(t) + Y_r v(t) \tag{33}$$

The state-variable form is

$$\frac{d}{dt}v(t) = -\frac{Y_r c}{Y_0(\epsilon_r - 1)2\Delta l}v(t) + \frac{2Y_r c}{Y_0(\epsilon_r - 1)2\Delta l}v_e^r(t)$$
$$\frac{d}{dt}i(t) = -\frac{Z_r c}{Z_0(\mu_r - 1)2\Delta l}i(t) + \frac{2Z_r c}{Z_0(\mu_r - 1)2\Delta l}v_m^r(t). \tag{34}$$

The final equations are

$$\frac{d}{dt}\begin{bmatrix}[v(t)]\\ [i(t)]\end{bmatrix} = \begin{bmatrix}-\alpha[U] & [0]\\ [0] & -\beta[U]\end{bmatrix}\begin{bmatrix}[v(t)]\\ [i(t)]\end{bmatrix} + \begin{bmatrix}2\alpha[U] & [0]\\ [0] & 2\beta[U]\end{bmatrix}\begin{bmatrix}[v_e^r(t)]\\ [v_m^r(t)]\end{bmatrix} \tag{35}$$

where $[U]$ is the 3×3 unitary matrix, $[v(t)]$ and $[i(t)]$ are the vectors containing the voltages and currents in x, y and z, $[v_a^r(t)]$ and $[v_n^r(t)]$ are the reflected voltages given by (20) and

$$\alpha = \frac{Y_r c}{Y_0(\epsilon_r - 1)2\Delta l} \quad \beta = \frac{Z_r c}{Z_0(\mu_r - 1)2\Delta l}. \tag{36}$$

B. Linear isotropic dispersive medium

In the case of a dispersive dielectric medium modeled by a first-order Debye approximation, the frequency domain permittivity function is [11]

$$\epsilon_r(\omega) = \epsilon_\infty + \frac{\epsilon_s - \epsilon_\infty}{1 + j\omega\tau_0}. \tag{37}$$

The relationship between E and D in this dispersive material will be modeled by the RC circuit shown in Fig. 4, with the analogies

$$C_1 = 2\Delta t(\epsilon_\infty - 1) \quad C_2 = 2\Delta t(\epsilon_s - \epsilon_\infty)$$
$$R = \frac{\tau_0}{2\Delta t(\epsilon_s - \epsilon_\infty).}$$

The state equation describing the circuit will be

$$\frac{d}{dt}[v_u] = [A][v_u] + [B][v_{eu}]$$
$$[v_{eu}^t] = [C][v_u] + [D][v_{eu}^r] \tag{38}$$

with

$$[A] = \begin{bmatrix}-\left(\frac{Y_r}{C_1} + \frac{1}{RC_1}\right) & \frac{1}{RC_1}\\ \frac{1}{RC_2} & -\frac{1}{RC_2}\end{bmatrix} \quad [B] = \begin{bmatrix}2\frac{Y_r}{C_1}\\ 0\end{bmatrix}$$
$$[C] = \begin{bmatrix}1\\ 0\end{bmatrix} \quad [D] = [-1] \quad [v_u] = \begin{bmatrix}v_u(t)\\ v_{u\text{aux}}(t)\end{bmatrix}$$
$$[v_{eu}^r] = [v_{eu}^r(t)] \tag{39}$$

where $u = x, y$ and z, $v_{u\text{aux}}(t)$ is an auxiliary variable used in the state-equation description of the system, Y_r is equal to 4 and v_{au}^r, v_{au}^t are the reflected and incident voltages at the input port of the network in the u direction. Therefore for each electric field component (x, y and z), a system of equations (39) has to be solved.

The dispersion analysis of TLM using state-variable approach shows that the timestep should be at least $\Delta t < \tau_0/100$ to obtain accurate results. If a small frequency shift is allowed

the limit can be decreased to $\Delta t < \tau_0/20$. This restriction applies to backward Euler and approximate trapezoidal discretization. In the case of second order materials, [12], the restriction is the same for the approximate trapezoidal case and it is worse for the backward Euler case. This rule of thumb for the discretization is valid as long as $\epsilon_r, \mu_r < 20$.

C. Linear anisotropic nondispersive material

Considering the anisotropic material with nondiagonal tensor

$$\boldsymbol{P} = [F]\boldsymbol{E} = ([\epsilon] - [U])\boldsymbol{E}$$
$$\boldsymbol{M} = [G]\boldsymbol{H} = ([\mu] - [U])\boldsymbol{H} \tag{40}$$

where

$$[\epsilon] = \begin{bmatrix} \epsilon_{xx} & \epsilon_{xy} & \epsilon_{xz} \\ \epsilon_{yx} & \epsilon_{yy} & \epsilon_{yz} \\ \epsilon_{zx} & \epsilon_{zy} & \epsilon_{zz} \end{bmatrix} \quad [\mu] = \begin{bmatrix} \mu_{xx} & \mu_{xy} & \mu_{xz} \\ \mu_{yx} & \mu_{yy} & \mu_{yz} \\ \mu_{zx} & \mu_{zy} & \mu_{zz} \end{bmatrix}$$
$$[U] = \begin{bmatrix} 1 & 0 & 0 \\ 0 & 1 & 0 \\ 0 & 0 & 1 \end{bmatrix}. \tag{41}$$

The constitutive state-equation is

$$2\Delta t \frac{d}{dt} \begin{bmatrix} v_x \\ v_y \\ v_z \\ i_x \\ i_y \\ i_z \end{bmatrix} = -4 \begin{bmatrix} [F]^{-1} & [0] \\ [0] & [G]^{-1} \end{bmatrix} \begin{bmatrix} v_x \\ v_y \\ v_z \\ i_x \\ i_y \\ i_z \end{bmatrix} - 8 \begin{bmatrix} [F]^{-1} & [0] \\ [0] & [G]^{-1} \end{bmatrix} \begin{bmatrix} v_{ex}^r \\ v_{ey}^r \\ v_{ez}^r \\ v_{mx}^r \\ v_{my}^r \\ v_{mz}^r \end{bmatrix}. \tag{42}$$

This relationship is obtained directly from (40) and (41) without the need for an equivalent circuit.

D. Nonlinear material

Consider the constitutive relationship of a nonlinear medium

$$P(t) = (\epsilon_r - 1)E(t) + \gamma(E(t))^3 \tag{43}$$

This is an example of a self-focusing material, because the effective dielectric constant increases with the amplitude of the wave. An electric field propagating in a waveguide loaded with a dielectric strip with this constitutive relationship tends to be more concentrated in the strip with increasing field values. Above certain power levels one observes the formation of spatial solitons in the guide.

The state-equation will be

$$\frac{d}{dt}v(t) = -\frac{Y_r}{Y_0[(\epsilon_r - 1)2\Delta l/c + 3\gamma(v(t))^2]}v(t) + \frac{2Y_r}{Y_0[(\epsilon_r - 1)2\Delta l/c + 3\gamma(v(t))^2]}v_a^r(t) \tag{44}$$

IV. Numerical Results

This technique was validated by comparing SCN TLM results for several materials:

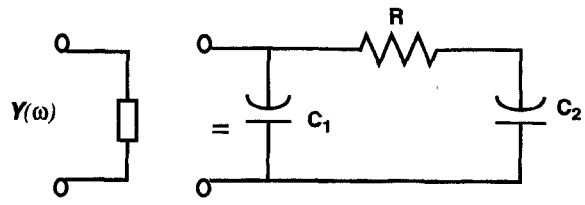

Fig. 4. Equivalent circuit model of a first-order Debye dielectric.

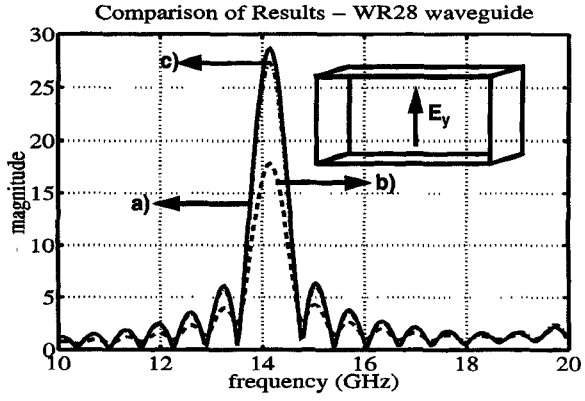

Fig. 5. The cutoff frequency of a WR-28 waveguide filled with dielectric. The frequency is obtained after a Fourier transform of the time domain response of an impulsive excitation of a cavity with the dimension of the guide. Results obtained with three different methods are compared. (a) stub-loaded SCN-TLM. (b) State-variable equations (backward Euler discretization). (c) State-variable equations (approximate trapezoidal discretization).

1) Comparison between cutoff frequency results obtained for a dielectric-filled isotropic waveguide using state-variable TLM and stub-loaded TLM. The example was a WR-28 waveguide (7.112 mm by 3.556 mm, backed by magnetic walls) with regular mesh with a discretization of $24 \times 12 \times 4$ filled with a dielectric with ϵ_r of 2.22. The first dominant mode of the cavity has the same frequency as the WR-28 guide. The results are shown in Fig. 5.
2) The calculation of the scattering parameters of a parallel plate waveguide with an air/dispersive material junction. The parallel plate waveguide was modeled by a mesh of 200 × 10 × 5 nodes (14.65 × 0.7325 × 0.366 25 mm) with the dielectric constant of $\epsilon_r = 1$ as shown in Fig. 6. In the first case (Fig. 7), the dispersive dielectric was modeled as a first order Debye medium with parameters $\epsilon_\infty = 1.8, \epsilon_s = 10.0$ and $\tau_0 = 9.4 \times 10^{-12}$ seconds. In the second case (Fig. 8), the dielectric was modeled as a second order Debye medium with $\epsilon_\infty = 20.0, \epsilon_s = 60.0$, $f_0 = 5$ GHz and $\delta = 0.3$. Both results were calculated using state-space equations discretized using backward Euler scheme.
3) The calculation of the cutoff frequencies of a sapphire filled WR-28 waveguide with the same discretization used in the first example. The permittivity tensor is

$$[\epsilon] = \begin{bmatrix} (\epsilon_u \cos^2\varphi + \epsilon_v \sin^2\varphi) & \frac{1}{2}(\epsilon_u - \epsilon_v)\sin 2\varphi & 0 \\ \frac{1}{2}(\epsilon_u - \epsilon_v)\sin 2\varphi & (\epsilon_v \cos^2\varphi + \epsilon_u \sin^2\varphi) & 0 \\ 0 & 0 & \epsilon_z \end{bmatrix} \tag{45}$$

where the dielectric was sapphire ($\epsilon_u = 9.34 \quad \epsilon_v = 11.49$), [8].

TABLE I
COMPARISON OF ANALYTICAL AND CALCULATED RESULTS FOR THE SAPPHIRE EXAMPLE

Analytical Cutoff Frequency	Axis Angle	SCN - TLM	Error (%)
6.2221 GHz	0°	6.21 GHz	0.19
6.5354 GHz	45°	6.57 GHz	0.53
6.9012 GHz	90°	6.90 GHz	0.02

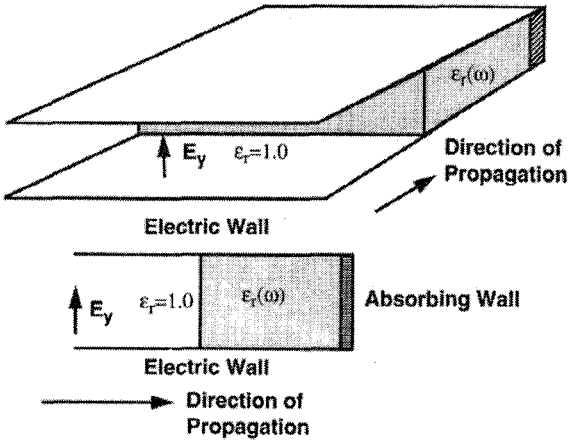

Fig. 6. Parallel plate waveguide half-filled with dispersive dielectric.

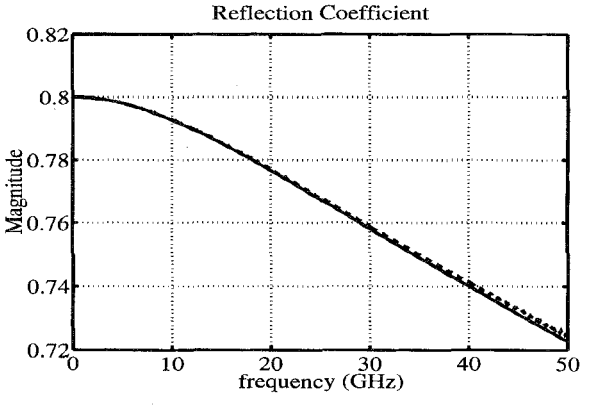

Fig. 7. Scattering parameters from an air/dispersive dielectric transition. Solid-line: exact result; dashed-line: result calculated with TLM. The maximum error over the whole frequency band is in the range of 0.4%.

The optical axis lies on the xy plane and was rotated by an angle φ with respect to the x axis. The problem was calculated for φ of 0°,45°, and 90° using backward Euler discretization. The comparison between the exact and calculated results is shown in Table I.

V. CONCLUSION

The technique presented in this paper can be used for modeling general constitutive relationships and requires few modifications to a TLM program. A general description of the medium relationships was obtained with equivalent node sources and the state-variable approach. The technique was validated by comparison with stub-loaded SCN results and exact solutions for the anisotropic case. Good agreement was observed in both cases.

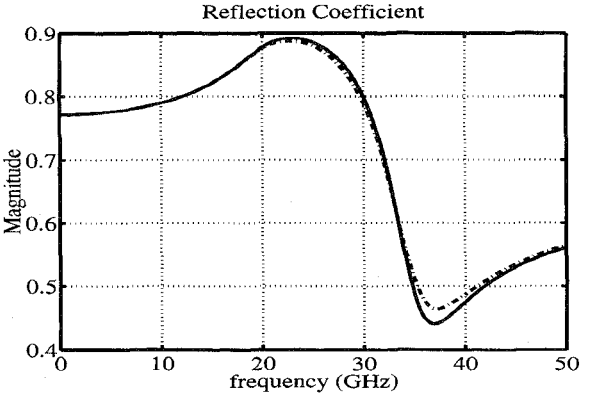

Fig. 8. Scattering parameters from an air/dispersive dielectric transition. Solid-line: exact result; dashed-line: result calculated with TLM. The RMS error over the whole frequency band is in the range of 3.0% (with a maximum of 6.0% at 36 GHz).

REFERENCES

[1] W. J. R. Hoefer, "The transmission line matrix method—theory and applications," *IEEE Trans. Microwave Theory Tech.*, vol. MTT-33, pp. 882–893, Oct. 1985.
[2] P. Russer, P. P. M. So, and W. J. R. Hoefer, "Modeling of nonlinear active regions in TLM," *IEEE Microwave Guided Wave Lett.*, vol. 1, pp. 10–13, Jan. 1991.
[3] L. de Menezes and W. J. R. Hoefer, "Modeling frequency dependent dielectrics in TLM," in *IEEE Antennas Propagat.-S Symp. Dig.*, June 1994, pp. 1140–1143.
[4] ——, "Modeling nonlinear dispersive media in 2-D-TLM," in *24th European Microwave Conference Proc.*, Sept. 1994, pp. 1739–1744.
[5] R. DeCarlo, *Linear Systems—A State-Variable Approach with Numerical Implementation.* Englewood Cliffs, NJ: Prentice-Hall, 1989.
[6] P. Naylor and R. Ait-Sadi, "Simple method for determining 3-D TLM nodal scattering in nonscalar problems," *Electronic Lett.*, vol. 28, pp. 2353–2354, Dec. 3, 1992.
[7] P. B. Johns, "A Symmetrical Condensed Node for the TLM Method," *IEEE Trans. Microwave Theory Tech.*, vol. MTT-35, n. 4, pp. 370–377, Apr. 1987.
[8] N. G. Alexoupoulos, "Integrated-circuits structures on anisotropic substrates," *IEEE Trans. Microwave Theory Tech.*, vol. MTT-33, no. 10, pp. 847–881, Oct. 1985.
[9] L. Chua, C. Desoer, and E. Kuh, *Linear and Nonlinear Circuits.* New York: McGraw-Hill, 1987.
[10] W. Press, B. Flannery, S. Teukolsky, and W. Vetterling, *Numerical Recipes in PASCAL.* Cambridge, MA: Cambridge Univ. Press, 1990, ch. 4.
[11] R. Luebbers, F. P. Hunsberger, K. Kunz, R. Standler, and M. Schneider, "A frequency-dependent finite-difference time domain formulation for dispersive materials," *IEEE Trans. Eletromagn. Compat.*, vol. 32, pp. 222–227, Aug. 1990.
[12] R. Luebbers and F. Hunsberger, "FDTD for nth-order dispersive media," *IEEE Trans. Antennas Propagat.*, vol. 40, pp. 1297–1301, Nov. 1992.

Leonardo R. A. X. de Menezes (S'89–M'91) was born in Brasilia, Brazil, in 1966. He received the degree in electrical engineering in 1990 and the M.Sc. degree in 1993, both from the University of Brasilia (UnB). He is the recipient of a scholarship of the Government of Brazil, and is currently working toward the Ph.D. degree in electrical engineering at the University of Victoria, Victoria B.C., Canada.

His research involves TLM modeling of general media, with emphasis on frequency-dependent and nonlinear dielectric material. His interests are in the areas of numerical modeling, radio frequency components and systems, semiconductor devices, and electromagnetic theory.

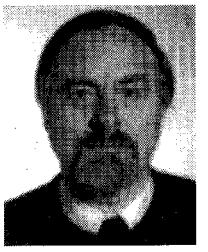

Wolfgang J. R. Hoefer (F'91) received the Dipl.-Ing. degree in electrical engineering from the Technische Hochschule Aachen, Germany, in 1965, and the D. Ing. degree from the University of Grenoble, France, in 1968.

During the academic year 1968 and 1969 he was a Lecturer at the Institut Universitaire de Technologie de Grenoble and a Research Fellow at the Institut National Polytechnique de Grenoble, France. In 1969, he joined the Department of Electrical Electrical Engineering, the University of Ottawa, Canada where he was a Professor until March 1992. Since April 1992 he has been the NSERC/MPR Tilted Industrial Research Chair in RF Engineering in the Department of Electrical and Computer Engineering, the University of Victoria, Canada. During sabbatical leaves he spent six months with the Space Division of AEG-Telefunken in Backnang, Germany (now ATN), and six months with the Electromagnetics Laboratory of the Institut National Polytechnique de Grenoble, France, in 1976 and 1977. In 1984 and 1985 he was a Visiting Scientist at the Space Electronics Directorate of the Communications Research Centre in Ottawa, Canada. He spent a third sabbatical year in 1990 and 1991 as a Visiting Professor at the Universities of Rome "Tor Vergata" in Italy, Nice-Sophia Antipolisi in France, and Munich (TUM) in Germany. His research interests include numerical techniques for modeling electromagnetic fields and waves, computer aided design of microwave and millimeter wave circuits, microwave measurement techniques, and engineering education. He is the co-founder and Managing Editor of the *International Journal of Numerical Modeling*.

Dr. Hoefer is a Fellow of the Advanced Systems Institute of British Columbia.